

This is the peer reviewed version of the following article: [Transl Res. . 2019 Feb;204:82-99.], which has been published in the final form at doi: 10.1016/j.trsl.2018.09.004. This article may be used for noncommercial purposes in accordance with Elsevier terms and conditions for use of self-archived version

# ORIGINAL ARTICLE

## A long-term treatment with taurine prevents cardiac dysfunction in *mdx* mice

ANTONIETTA MELE<sup>1</sup>, PAOLA MANTUANO<sup>1</sup>, MICHELA DE BELLIS, FRANCESCO RANA,  
FRANCESCA SANARICA, ELENA CONTE, MARIA GRAZIA MORGESE, MARIA BOVE,  
JEAN-FRANCOIS ROLLAND, ROBERTA FRANCESCA CAPOGROSSO, SABATA PIERNO,  
GIULIA MARIA CAMERINO, LUIGIA TRABACE, and ANNAMARIA DE LUCA

BARI, FOGGIA, AND BRESCO (MILAN), ITALY

Taurine is an amino acid abundantly present in heart and skeletal muscle. Duchenne muscular dystrophy (DMD) is a genetic disorder in which the absence of dystrophin leads to skeletal muscle wasting and heart failure. An altered taurine metabolism has been described in dystrophic animals and short-term taurine administration exerts promising amelioration of early muscular alterations in the *mdx* mouse model of DMD. To reinforce the therapeutic and nutraceutical taurine potential in DMD, we evaluated the effects of a long-term treatment on cardiac and skeletal muscle function of *mdx* mice in a later disease stage. Taurine was administered in drinking water (1 g/kg/day) to wt and *mdx* mice for 6 months, starting at 6 months of age. Ultrasonography evaluation of heart and hind limb was performed, in parallel with *in vivo* and *ex vivo* functional tests and biochemical, histological and gene expression analyses. 12-month-old *mdx* mice showed a significant worsening of left ventricular function parameters (shortening fraction, ejection fraction, stroke volume), which were significantly counteracted by the taurine treatment. In parallel, histologic signs of damage were reduced by taurine along with the expression of proinflammatory myocardial IL-6. Interestingly, no effects were observed on hind limb volume and percentage of vascularization or on *in vivo* and *ex vivo* muscle functional parameters, suggesting a tissue-specific action of taurine in relation to the disease phase. A trend toward increase in taurine was found in heart and quadriceps from treated animals, paralleled by a slight decrease in *mdx* mice plasma. Our study provides evidences that taurine can prevent late heart dysfunction in *mdx* mice, further corroborating the interest on this amino acid toward clinical trials. (Translational Research 2018; 000:1–18)

**Abbreviations:** CK = creatine kinase; CO, cardiac output; cardiac output; Cs = citrate synthase; Cox4i1 = cytochrome c oxidase subunit IV isoform 1; DGC = dystrophin-glycoprotein complex; DIA = diaphragm; DMD = Duchenne muscular dystrophy; EDL = extensor digitorum longus; Eef2 = eukaryotic translation elongation factor 2; EF = ejection fraction;

<sup>1</sup>These authors equally contributed to the work.

From the Section of Pharmacology, Department of Pharmacy - Drug Sciences, University of Bari “A. Moro”, Bari, Italy; Department of Experimental and Clinical Medicine, Faculty of Medicine, University of Foggia, Foggia, Italy; Axxam, S.p.A, Openzone Science Park, Bresso (Milan), Italy.

Submitted for Publication April 12, 2018; received submitted September 6, 2018; accepted for publication September 25, 2018.

Reprint requests: Annamaria De Luca, Section of Pharmacology, Department of Pharmacy - Drug Sciences, University of Bari “Aldo Moro”, Via E. Orabona 4 – Campus, 70125 Bari, Italy; e-mail: annamaria.deluca@uniba.it.

1931-5244/\$ - see front matter

© 2018 Elsevier Inc. All rights reserved.

<https://doi.org/10.1016/j.trsl.2018.09.004>

GAPDH = glyceraldehyde-3-phosphate dehydrogenase; Slc6a6 = solute carrier family 6 (neurotransmitter transporter; taurine) member 6; GC = gastrocnemius muscle; IL-6 = interleukin 6; LDH = lactate dehydrogenase; NF- $\kappa$ B = nuclear factor kappa-light-chain-enhancer of activated B cells; PV = percentage of vascularization; ROS = reactive oxygen species; Rplp0 = ribosomal protein, large, P0; SF = shortening fraction; SV = stroke volume; TauT = taurine transporter

## AT A GLANCE COMMENTARY

Mele A, et al.

### Background

Duchenne muscular dystrophy (DMD) is a genetic disorder in which the absence of dystrophin leads to skeletal muscle wasting and heart failure.

Skeletal and cardiac muscles of both DMD patients and dystrophic *mdx* mice show an alteration of taurine levels and metabolism which contributes to the progression of muscle degeneration and cardiac dysfunction.

### Translational Significance

By a cardiac ultrasonography evaluation, we demonstrate that long-term taurine administration prevents late cardiac dysfunction in *mdx* mice, supporting the translational potential of taurine as therapeutic agent in DMD to delay the left ventricular failure which is the main cause of death in young patients.

## INTRODUCTION

Taurine (2-aminoethane-sulfonic acid) is a natural, sulfur-containing amino acid that is found free in most of mammalian tissues, where it exerts multiple physiological functions acting as osmolyte, ion channels modulator, regulator of  $\text{Ca}^{2+}$  homeostasis, as well as antioxidant and anti-inflammatory compound.<sup>1–4</sup> In heart and skeletal muscle, taurine is present in very high concentrations ensured by a specific  $\text{Na}^+/\text{Cl}^-$  dependent transport system (TauT) which is ubiquitously expressed in mammalian tissues.<sup>5</sup> In line with the key role of taurine for tissue function, pharmacologic or genetic inhibition of TauT transporter in adult rats markedly reduces the taurine levels in both heart and skeletal muscle leading to clear structural abnormalities (atrophy, necrosis), reduced exercise performance and a slow-to-fast metabolic shift, along with an overt cardiomyopathy.<sup>6–8</sup> In fast twitch extensor digitorum longus muscle (EDL) muscle, taurine depletion is accompanied by marked alteration of excitation-contraction coupling, with a shift of the calcium sensitive mechanical threshold toward more negative potentials, an index of deregulated cytosolic calcium and a decrease in macroscopic conductance to  $\text{Cl}^-$  ions (gCl).<sup>9,10</sup> A suffering in retaining a proper tissue

amount of taurine, along with alterations in taurine metabolism may occur in conditions of progressive muscle degeneration, such as in Duchenne muscular dystrophy (DMD). DMD is a fatal genetic disease caused by the absence of the protein dystrophin, a subsarcolemmal component of the dystrophin-glycoprotein complex that plays a key role in both membrane integrity and mechanotransduction signaling. The same biochemical defect occurs in the *mdx* mouse, the most widely used animal model for preclinical studies on DMD.<sup>11</sup> The lack of dystrophin progressively leads to skeletal muscle wasting and fibrosis via a complex cascade of pathogenic processes, including increased membrane permeability and altered calcium homeostasis, oxidative stress and chronic inflammation, activation of profibrotic pathways followed by inefficient regeneration and necrosis.<sup>12</sup> Various evidences support that taurine level can be altered in dystrophic muscles in relation to early degeneration and regeneration cycles and such an alteration may account for some of the hallmarks typically observed, such as the deregulated calcium homeostasis and the mechanosensitive impairment of excitation-contraction coupling mechanism.<sup>13–16</sup> We have extensively exploited the effect of taurine as a potential early countermeasure of muscle alterations observed in the exercised *mdx* mouse; this model is characterized by a worsening of pathology-related readouts and shows features more closely resembling those of a taurine-depleted condition. Importantly, early taurine administration (1 g/kg/day, orally for 4–8 weeks), matching the age at which acute pathology phase occurs, contrasted the typical *in vivo* weakness and ameliorated calcium homeostasis and excitation-contraction coupling mechanism, via a direct action on ion channel function; this was accompanied by a tissue increase of taurine level.<sup>14,15,17</sup> Interestingly, taurine was also able to contrast typical myofiber alterations via acute *in vitro* application, while *in vivo* it exerted a synergistic effect on sensitive parameters with  $\alpha$ -methylprednisolone, a gold standard therapy in DMD patients.<sup>14,15,17</sup> More recently, we confirmed that the action of taurine in exercised *mdx* mice was paralleled by a reduction of dihydroethidium staining of superoxide anion and of activated NF- $\kappa$ B positive myofibers, along with an improved muscle histologic profile.<sup>18</sup> These findings are in line with the view of taurine being beneficial via a marked antioxidant and anti-inflammatory action; in fact, the Arthur's group found a reduction of thiol oxidation, of myeloperoxidase and of neutrophils activity in young *mdx* mice and in the golden retriever muscular dystrophy

canine model of DMD treated with taurine or its precursor 2-oxothiazolidine-4 carboxylate.<sup>19–21</sup>

The large body of preclinical evidences from independent research groups obtained with early and short-term taurine exposure has raised attention for clinical studies in DMD. This also in consideration that taurine is a ready-to-use cheap compound with a favorable safety profile in humans, both adults and children,<sup>4,22</sup> being already used as nutraceutical supplement as well as in energy drinks and in neonatal formulas.<sup>23</sup> In order to reinforce the translational potential of taurine as therapeutic agent in DMD, it is pivotal to assess its efficacy and safety over long-term exposure, paying particular attention on its potential cardioprotective action. In fact, a cardiac dysfunction progressively occurs in DMD boys, with severe dilated cardiomyopathy and left ventricular failure being present in almost all boys around the 18<sup>th</sup> year of age, and largely contributing to death for cardiorespiratory failure.<sup>24,25</sup> As described above, appropriate taurine transport and concentration are also required for contractile efficiency of the heart<sup>3</sup>; accordingly, taurine has been found to have beneficial effect on a variety of preclinical and clinical conditions characterized by cardiac suffering, such as myocardial ischemia-reperfusion injury, congestive heart failure, hypertension, atherosclerosis, and diabetic cardiomyopathy.<sup>26,27</sup>

In the *mdx* mouse model, cardiac failure is a late phenomenon that appears around the 9<sup>th</sup> month of age<sup>28</sup> and the effects of taurine on late stage of pathology have never been investigated up to now. The present study was aimed at evaluating the potential effectiveness of a long-term treatment with taurine (6 months) in preventing late cardiac failure in *mdx* mice. In parallel, we assessed if the long-term administration of taurine maintains general safety as well as the efficacy observed in the short-term treatment on disease-sensitive skeletal muscle readouts. To these aims, we presently performed an ultrasonography evaluation of heart and skeletal muscle structure and function, in parallel with the assessment of behavioral *in vivo* parameters that are indices of mouse weakness and fatigability. *Ex vivo* studies were also performed to assess the impact of taurine treatment on muscle function and tissue histopathology, as well as on plasma and tissue biomarkers of damage and taurine action.

## MATERIALS AND METHODS

All the experiments were conducted in conformity with the Italian Guidelines for Care and Use of Laboratory Animals (D.L.116/92), and with the European Directive (2010/63/UE). The study has been approved by national ethic committee for research animal welfare of the Italian Ministry of Health (authorization

numbers: 815 and 816/2017-PR). Most of the experimental protocols conform to the standard operating procedures (SOPs) for preclinical tests in *mdx* mice, available on the TREAT-Neuromuscular Disease (TREAT-NMD) network website (<http://www.treat-nmd.eu/research/preclinical/dmd-sops/>).

**Animal groups and drug treatment.** A total of 26 male mice, 13 wild type (wt; C57BL/10ScSn/J) and 13 *mdx* mice (C57BL/10ScSn-*Dmd*<sup>mdx</sup>/J) of 26 weeks of age (~6 months) were purchased from The Jackson Laboratory (USA, distributed by Charles River, Calco, Italy) to perform the study. All mice were acclimatized for 1 week in the animal facility, prior to the beginning of the experimental protocol. For each genotype, the animals were divided into cages based on mean body weight; then, they were randomly assigned to each experimental group (n = 7 wt or *mdx* mice treated with taurine 1 g/kg/day; n = 6 wt or *mdx* mice treated with vehicle). Taurine (Sigma-Aldrich, Italy) was formulated in filtered tap water and was administered orally at a dose of 1 g/kg/day, according to mice mean body weight and to daily water consumption. Water consumption was carefully monitored throughout. Mice were treated for 6 months, from 6 to 12 months of age. The dose of taurine was chosen based on our previous *in vivo* studies on *mdx* mice.<sup>15,17,18</sup> All mice were maintained on a controlled diet (for composition see Capogrosso et al., 2018<sup>29</sup>), with a daily amount of chow of 4–5 g/mouse. For the whole duration of the study, no signs of stress (lack of appetite, body weight loss, hair loss, stereotypic or aggressive behavior, etc.) or macroscopic alterations of vital functions were observed in treated or untreated animals of both genotypes.

**In vivo parameters of muscle strength and fatigability.** At the beginning (6 months of age) and at the end (12 months of age) of the treatment protocol, all animals were monitored for body weight and forelimb strength by means of a grip strength meter (Columbus Instruments, Columbus, Ohio), according to TREAT-NMD SOPs. The values of both absolute and normalized (to body weight) maximal forelimb force were used for statistical analysis.<sup>15,17,30</sup> At the same time points, an acute exercise resistance test was performed to assess *in vivo* fatigue. The animals were made running on a horizontal treadmill (Columbus Instruments) for 5 minutes at 5 m/min, then increasing the speed of 1 m/min each minute. The total distance (in meters) ran by each mouse until exhaustion was calculated.<sup>15,17,30</sup>

**Ultrasonography evaluations.** At the same time points (6 and 12 months of age) of *in vivo* force and fatigability assessments, an ultrasonography evaluation of cardiac and skeletal muscle structure and function was performed. At least 48 hours elapsed since the end of

previously described *in vivo* tests, in order to avoid any additional source of stress for the animals that could potentially influence the outcome of the ultrasound procedure. Ultrasonography experiments were conducted using the ultra-high frequency ultrasound biomicroscopy system Vevo 2100 (VisualSonics, Toronto, ON, Canada), which allows multiple images acquisition modes.

According to TREAT-NMD SOPs, the animals were properly prepared prior to each imaging session to allow an optimal image acquisition. Each mouse was anesthetized via inhalation (induction with ~3% isoflurane and 1.5% O<sub>2</sub> l/min, then constantly maintained via nose cone at ~2% isoflurane and 1.5% O<sub>2</sub>) and placed on a thermostatically controlled table (kept at 37°C). This latter was equipped with 4 copper leads which allow the monitoring of both heart and respiratory rate of the mouse to minimize any physiological variation. Also, body temperature was monitored during the whole imaging session using a rectal probe. A petroleum-based lubricant was used to cover the eyes in order to prevent the drying of the area. The thorax and the hind limb of the animal were properly shaved with depilatory cream to avoid any interference during images acquisition and a small amount of pre-heated ultrasound gel was applied between the animal skin and the probe to guarantee a proper image recording. At the end of the procedure, the anesthetic influx was discontinued, and each animal was first cleaned with water and then returned to its cage in the animal facility after briefly recovering from anesthesia in an oxygenated box.<sup>31,32</sup>

**Acquisition of cardiac parameters.** Echocardiography was performed on wt and *mdx* mice in bi-dimensional mode (B-Mode) and mono-dimensional mode (M-Mode), by using a high-resolution transducer at a frequency of 40 MHz (MS550). Images were acquired in modified parasternal long axis (PLAX) view, with the animal placed in supine position. Briefly, the left ventricle (LV) M-Mode trace was used to measure ejection fraction (EF, %), shortening fraction (SF, %), stroke volume (SV, µl) and cardiac output (CO, ml/min).<sup>33</sup> Left ventricular diastolic and systolic chamber internal diameter (LVID<sub>(d)</sub>; LVID<sub>(s)</sub>), posterior wall thickness (PLW<sub>(d)</sub>; PLW<sub>(s)</sub>), intraventricular septum (IVS<sub>(d)</sub>; IVS<sub>(s)</sub>) were also measured.

**Ultrasound evaluation of the hind limb.** For the acquisition of hind limb images from wt and *mdx* mice, each animal, properly anesthetized, was placed in ventral decubitus position. The hind limbs were positioned strictly parallel to the body, with each foot forming an angle of 90° with the hind limb. After the application of the ultrasound gel, a 3-dimensional (3D) volume scan of the hind limbs was acquired by translating the ultrasound probe parallel to the long axis of the hind

limb.<sup>31,32</sup> The multiple 2-dimensional (2D) images were acquired at regular intervals in Power Doppler mode by using a MS250 probe at a frequency of 21 MHz, characterized by lateral and axial resolutions of 165 and 75 µm, respectively. At the end of the procedure, 3D images were reconstructed from previously collected multiple 2D frames and visualized with VisualSonics 3D software. This allowed to calculate both the total volume (in mm<sup>3</sup>) and the percentage of vascularization (PV%) of the hind limb.

**Ex vivo procedures.** At the end of *in vivo* functional and ultrasound measurements, the *ex vivo* experimental phase started. Due to the time-consuming nature of some experiments, no more than 2 animals could be sacrificed *per* day, thus a window of 3–4 weeks should be considered until the end of these procedures. The animals continued to be treated until the day of sacrifice.

**Muscle preparations, organ biopsies, and blood collection.** Prior to microsurgical excision of muscles and organs, all mice were anesthetized intraperitoneally with a ketamine (100 mg/kg) and xylazine (16 mg/kg) cocktail; ketamine was additionally administered alone, at a dose of 30 mg/kg, to ensure a longer and deeper sedation, if required. This procedure was necessary to guarantee a normal blood circulation during the excision of muscles and organs, so to preserve unaltered their structural and functional features. A strip of right hemi-diaphragm (DIA) and the EDL muscle of the left hind limb were carefully removed with intact tendons on both ends, and then rapidly placed in muscle baths for contractile recordings. Quadriceps muscle from the right hind limb, heart (atria, after blood collection), brain and a portion of the liver were accurately dissected, weighed and rapidly homogenized in 0.1N perchloric acid using Potter-Elvehjem glass tissue homogenizers. Homogenized tissues were then centrifuged at 10,300 g for 60 minutes at 4°C and supernatant was stored at –80°C for further high performance liquid chromatography (HPLC) analysis. Left gastrocnemius muscle (GC) and the apex of the heart were carefully dissected, embedded in a small amount of Tissue-Tek O.C.T. (Bio-Optica, Milan, Italy) and immersed in isopentane cooled with liquid nitrogen for 40–60 seconds in a slightly stretched position; frozen samples were stored at –80°C until further histologic analysis. A portion of frozen ventricle was used for Real-time polymerase chain reaction (PCR) experiments. Blood collection was performed via cardiac puncture of LV with a heparinized insulin syringe. Plasma samples were obtained after centrifugation for 10 minutes at 3000 g at 4°C, within 30 minutes after blood collection. Fresh plasma aliquots (~150 µl) were used to measure creatine kinase (CK) and lactate

dehydrogenase (LDH) levels by spectrophotometric assays. In parallel, plasma aliquots of  $\sim 50 \mu\text{l}$  were stored at  $-20^\circ\text{C}$  for further HPLC analysis.

**Isometric and eccentric contraction recordings on isolated muscles.** A strip of right hemi-DIA (no more than 4-mm wide) was cut from the excised muscle and then firmly tied at the rib and at the central tendon. EDL muscle from the left hind limb was securely tied with silk suture 6–0 to the proximal and distal tendons during dissection.<sup>34</sup> Two loops were made at the end of the sutures to place the muscles into recording chambers containing a normal physiological Ringer's solution (in mM): NaCl 148, KCl 4.5, CaCl<sub>2</sub> 2.0/2.5, MgCl<sub>2</sub> 1.0, NaH<sub>2</sub>PO<sub>4</sub> 0.44, NaHCO<sub>3</sub> 12.0, glucose 5.55, pH 7.2 – 7.4,  $27 \pm 1^\circ\text{C}$ ) continuously gassed with a mixture of 95% O<sub>2</sub> and 5% CO<sub>2</sub>. EDL muscle was placed in a horizontal muscle bath (mod. 809B-25, ASI, Aurora, Ontario, Canada) fixed by one tendon to chamber hook, while the other tendon was fixed to a Dual-Mode Lever System 1N force transducer (mod. 300C LR, ASI), connected to a proper interface and data acquisition system (605A with Dynamic Muscle Control v5.415, ASI). The diaphragm strip was placed in a vertical bath with the central tendon fixed to a chamber hook and the rib fixed to a force transducer (FORT25, WPI Inc, Florida), connected to a TCI 102 interface with a MP100 acquisition unit and AcqKnowledge v.3.8 software (Biopac Systems, Santa Barbara, California). Electrical field stimulation was obtained by 2 axial platinum electrodes closely flanking the muscles, which were connected to a stimulator (EDL: 701C High-Power, Bi-Phase Stimulator, ASI; DIA: LE 12406, 2Biological Instruments, VA, Italy). After a 30-minute equilibration, muscle preparations were stretched to their optimal length (L<sub>0</sub>), measured with an external calliper. L<sub>0</sub> represents the length producing the maximal single contraction (twitch) in response to a 0.2 ms square wave 40–60 mV pulse. Maximal twitch tension was obtained as the mean value from 5 single twitches elicited by pulses of 0.2 ms, every 30 seconds. Tetanic contractions were elicited by applying trains of 350 ms and 450 ms (for EDL and DIA, respectively) of 2.0 ms pulses at increasing frequencies (10–200 Hz), every 2 minutes. The maximal tetanic force was usually elicited at 180/200 Hz for EDL, and at 140/180 Hz for DIA. In addition, EDL muscles underwent a train of 10 eccentric contractions elicited at 120 Hz for 500 ms, every 30 seconds. For each stimulation, an initial isometric contraction was elicited for 300 ms, followed by a stretch of 10% L<sub>0</sub> at a speed of 1L<sub>0</sub> s<sup>-1</sup> imposed for the last 200 ms. The progressive decay in isometric force at 5<sup>th</sup> and 10<sup>th</sup> pulse, as well as the recovery after 4 minutes and 30 minutes from eccentric protocol, were calculated as described in previous work.<sup>35,36</sup> At the end of the experiments, tendons were removed

and muscles were blotted dry with filter paper and weighed. Data were analyzed using AcqKnowledge software v3.8 (Biopac Systems) for DIA and Dynamic Muscle Analysis software v5.201 (ASI) for EDL, to obtain muscle contraction kinetics (time to peak twitch and half relaxation time, in ms) and absolute values of maximal twitch (P<sub>tw</sub>) and tetanic (P<sub>0</sub>) tension. Absolute data were expressed in mN. Then, absolute values were normalized by muscle cross-sectional area according to the equation  $sP = P/(Mass/Lf^2D)$  where P is absolute tension, Mass is the muscle mass, D is the density of skeletal muscle (1.06 g/cm<sup>3</sup>); Lf was determined by multiplying L<sub>0</sub> by previously determined muscle length to fiber length ratios (DIA = 1; EDL = 0.44).<sup>36–39</sup>

**Histologic evaluation of skeletal and cardiac muscle.** Serial cross-sections (8  $\mu\text{m}$  thick) of previously frozen GC and cardiac muscle samples were transversally cut into a cryostat microtome set at  $-20^\circ\text{C}$  (HM 525 NX, Thermo Fisher Scientific, Massachusetts) and stained with hematoxylin and/or eosin to calculate the total area of damage (necrosis, inflammation and non-muscle areas). On GC sections, the percentage of regenerating and/or regenerated myofibers, showing central nuclei (centrally nucleated fibers) were also evaluated. Morphological features of the muscles were identified using digital images of stained sections, acquired using a bright-field microscope (CX41, Olympus, Rozzano, Italy) and an image capture software (Image J, Olympus). Morphometric analysis was performed on at least 5 fields (10X magnification) from each muscle section and at least 5 animals per group were assessed.<sup>18,29,39</sup>

**Isolation of total RNA, reverse transcription and Real-time PCR.** Real-time PCR experiments were performed according to the MIQE guidelines for qPCR, as published.<sup>40</sup> Total RNA was isolated from heart muscles by RNeasy Fibrous Tissue Mini Kit (Qiagen, Valencia, California; C.N.74704) and quantified by spectrophotometry (ND-1000 NanoDrop, Thermo Scientific, Waltham, Massachusetts). To perform reverse transcription, for each sample, 400 ng of total RNA was added to 1  $\mu\text{l}$  dNTP mix 10 mM each (Roche N.C. 11277049001), 1  $\mu\text{l}$  RandomHexamers 50  $\mu\text{M}$  (Life-Technologies C.N. n808-0127) and incubated at 65°C for 5 minutes. Afterward, 4  $\mu\text{l}$  5°X First Standard Buffer (lifetechnologies C.N. Y02321), 2  $\mu\text{l}$  0.1 M DTT (life-technologies C.N. Y00147) and 1  $\mu\text{l}$  Recombinant RNasin Ribonuclease Inhibitor 40 U/ $\mu\text{l}$  (Promega, C.N. N2511) were added and incubated at 42°C for 2 minutes. Then, 1  $\mu\text{l}$  Super Script II Reverse Transcriptase 200 U/ $\mu\text{l}$  (Life-Technologies C.N. 18064-014) was added, and the samples were incubated at 25°C for 10 minutes, at 42°C for 50 minutes and at 70°C for 15 minutes. Real-time PCR was performed in duplicate using the Applied Biosystems Real-time

PCR 7500 Fast system, MicroAmp Fast Optical 96-Well Reaction Plate 0.1 mL (Life-Technologies C.N. 4346906) and MicroAmp Optical Adhesive Film (life-technologies C.N. 4311971). The setup of reactions consisted 8 ng of cDNA, 0.5  $\mu$ L of TaqMan Gene Expression Assays, (Life-Technologies), 5  $\mu$ L of Taq-Man Universal PCR master mix No AmpErase UNG (2x) (Life-Technologies C.N. 4324018) and Nuclease-Free Water not DEPC-Treated (Life-Technologies C. N. AM9930) for a final volume of 10  $\mu$ L. The RT-Taq-Man-PCR conditions were as follows: step 1: 95°C for 20 seconds; step 2: 95°C for 3 seconds; and step 3: 60° C for 30 seconds; steps 2 and 3 were repeated 40 times. The results were compared with relative standard curve obtained by 5 points of 1:4 serial dilutions. TaqMan Hydrolysis primer and probe gene expression assays were ordered by Life-Technologies with the following Assay IDs: eukaryotic translation elongation factor 2 (Eef2): Mm01171434\_g1, ribosomal protein, large, P0 (Rplp0): Mm00725448\_s1, glyceraldehyde-3-phosphate dehydrogenase (GAPDH):Mm99999915\_g1, solute carrier family 6 (neurotransmitter transporter, taurine) member 6 (Slc6a6): Mm00436909\_m1, interleukin 6 (Il6): Mm00446190\_m1, citrate synthase (Cs) : Mm00466043\_m1, cytochrome c oxidase subunit IV isoform 1 (Cox4i1): Mm01250094\_m1. The mRNA expression of the genes was normalized to the best housekeeping gene, which resulted to be Rplp0, selected among Eef2, GAPDH and Rplp0 by GeNorm, NormFinder, and BestKeeper softwares.<sup>40,41</sup>

**HPLC determination of taurine content in skeletal muscle, internal organs, and plasma.** Taurine levels in quadriceps, heart, brain and liver homogenates and in plasma samples were measured by HPLC using ODS-3 column (150  $\times$  4.6 mm, 3  $\mu$ m; INERTSIL) with fluorescence detection after derivatization with ophthalaldehyde and/or mercaptopropionic acid (emission length: 4.60 nm; excitation length: 3.40 nm). The mobile phase gradient consisted of sodium acetate buffer (50 mM, pH 6.95) with methanol increasing linearly from 2% to 30% (v/v) over 40 minutes. Flow rate was maintained at 0.5 ml/min by a pump (JASCO, Tokyo, Japan). Results were analyzed by Borwin software (version 1.50; Jasco) and the substrate concentration was expressed as  $\mu$ mol/mg of tissue and as  $\mu$ M for plasma.<sup>42</sup>

**Plasma levels of biochemical markers of muscle damage.** The spectrophotometric determination of the levels of CK and LDH in fresh plasma samples was performed according to the instructions of commercial diagnostic kits (CK NAC LR for creatine kinase and LDH LR for lactate dehydrogenase, respectively; SGM Italia, Rome, Italy). For both assays, the instrument (Ultrospec 2100 pro,

Amersham Biosciences, UK) was set to a wavelength of 340 nm, at a temperature of 37°C.

**Statistical analysis.** All data are expressed as the mean  $\pm$  the standard error of the mean (S.E.M.). Multiple statistical comparison among groups was performed by one-way analysis of variance (ANOVA), followed by Bonferroni post hoc correction, to better evaluate intra- and inter-group variability and to avoid false positives. If necessary, a direct comparison between data pairs was made by unpaired Student's *t* test to assess intra- and inter-genotype differences. The recovery score, an objective index to assess the effect of a drug treatment on a given parameter, was calculated according to TREAT-NMD SOPs (<http://www.treat-nmd.eu/research/preclinical/dmd-sops/>) with the formula:

$$\text{Recovery score} = [\text{mdx treated}] - [\text{mdx untreated}] / [\text{wild type}] - [\text{mdx untreated}] \times 100$$

## RESULTS

**Body weight and water intake.** All mice were non-invasively and longitudinally monitored for body weight and water intake. The results for body weight measurements at 6 and 12 months of age are reported in Fig 1, A. At 6 months of age, *mdx* mice resulted significantly heavier than wt mice, in agreement with our previous studies.<sup>15,30,36,38</sup> Taurine administration did not induce any modification in the body weight of *mdx* mice, while a significant increase was found in 12-month-old wt animals, with respect to untreated ones (Fig 1, A). The determination of body weight was also important to calculate the dose of taurine assumed by each mouse with drinking water.<sup>29</sup> The water intake by wt and *mdx* mice treated with taurine assessed at regular time intervals and normalized to body weight was not significantly different (Fig 1, B). The calculated dose of taurine assumed by the mice during the treatment was in a range between 0.8 and 1.1 g/kg, which was in line with the expected dose of 1 g/kg. The slight variations observed could be due to an occasional under- or over-estimation of water consumption.

**Effect of long-term taurine administration on left ventricular function.** Heart structure and function were evaluated by echocardiography in both wt and *mdx* mice, at the beginning and at the end of the treatment protocol. Sample images acquired during cardiac ultrasound are shown in Fig 2, A and B. No significant differences between wt and *mdx* mice were observed at 6 months of age for the main parameters related to left ventricular function: SV,  $\mu$ l (Fig 2, C), CO, ml/min (Fig 2, D), SF, % (Fig 2, E) and EF, % (Fig 2, F). At 12 months of age, untreated *mdx* mice showed a significant reduction of SF ( $-22.8\%$ ), EF ( $-18.4\%$ ) and SV ( $-29\%$ ) with respect to untreated wt mice, which is in line with the development of cardiac impairment around 9 months of age, already reported in dystrophic animals<sup>28</sup> (Fig 2, C, E, F). A slight, but non-significant, trend toward reduction was also observed for CO in *mdx* mice (Fig 2, D). Interestingly, the long-term treatment with taurine exerted a protective action on these indices in *mdx* mice, inducing a significant amelioration of SF, EF, and SV with respect to their untreated counterparts. These values resembled those found in wt mice, in which taurine did not induce any significant modifications (Fig 2, C, E, and F). No significant variations were also observed for the CO parameter in either wt or *mdx* mice (Fig 2, D). In addition, no significant difference among groups was found at any age for structural parameters, such as left ventricular diastolic and systolic posterior wall thickness (PLW<sub>d</sub>; PLW<sub>s</sub>),

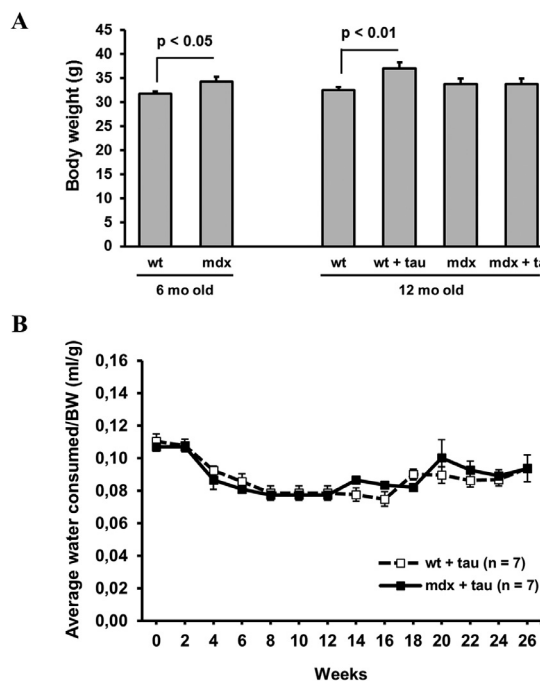


**Fig 1.** Evaluation of body weight (BW) and water intake. In A are shown body weight measurements at the beginning (6 mo old) and at the end (12 mo old) of the treatment for treated/untreated wild type (wt) and *mdx* mice. Each bar is the mean  $\pm$  SEM from 6 to 7 mice per group. A significant difference among groups was found at 12 months of age by ANOVA analysis ( $F > 3.14$ ;  $P < 0.05$ ). Intra- and inter-genotype significances found by unpaired Student's t test are indicated above the bars. In B is shown the average water consumption normalized on body weight over time (every 2 weeks) for wt and *mdx* mice treated with taurine.

diastolic and systolic internal diameter (LVID<sub>(d)</sub>; LVID<sub>(s)</sub>), or diastolic and systolic intraventricular septum (IVS<sub>(d)</sub>; IVS<sub>(s)</sub>) (data not shown).

**Effect of long-term taurine treatment on hind limb volume and percentage of vascularization.** At the same time points, all animals underwent an ultrasonographic assessment of hind limb volume ( $\text{mm}^3$ ) and percentage of vascularization (PV%, Fig 3). Representative 3D images of hind limb ultrasonographic volume and PV% in wt mice (left panel) and *mdx* mice (right panel) are shown in Fig 3A. At 6 months of age, untreated *mdx* mice showed a significant enhancement of the hind limb volume (7%) with respect to untreated wt mice, that is in line with the skeletal hypertrophy characterizing *mdx* mice at this stage of myopathy.<sup>11,43</sup> No significant differences in the hind limb volume were observed among the experimental groups at 12 months (Fig 3, B). For PV%, a significant time-dependent increase was observed both for wt and *mdx* animals at 12 months with respect to 6 months of age. No effects were induced by taurine treatment on any of these parameters in either wt and *mdx* mice (Fig 3, C).

**Effects of long-term taurine treatment on *in vivo* indices of muscle strength and fatigability.** In parallel with ultrasonography, all mice were monitored for *in vivo* forelimb strength and exercise performance. The values at 6 and 12 months of age are reported in Fig 4. Considering the variations in the body weight, the value of absolute forelimb force of each mouse was normalized to its body weight (Fig 4, A). According to previous studies, values of normalized force from dystrophic mice were significantly lower than those of wt mice, both at 6 and 12

months of age. Surprisingly, the long-term treatment with taurine did not exert any positive effect on this parameter in the two genotypes, as well as on exercise performance during the exhaustion test on treadmill (Fig 4, B).

**Effect of long-term taurine administration on *ex vivo* contraction of isolated muscles.** At the end of *in vivo* recordings, the muscle-specific effects of long-term taurine treatment were evaluated by *ex vivo* isometric and eccentric contraction recordings on isolated DIA and EDL muscles from wt and *mdx* mice. As expected, DIA specific twitch (sPt<sub>w</sub>, kN/m<sup>2</sup>) and tetanic (sP0, kN/m<sup>2</sup>) force values from *mdx* mice were significantly lower compared to those of wt (Fig 5, A and B).<sup>36</sup> In EDL muscle, the significant difference between genotypes was maintained for sPt<sub>w</sub>, but not for sP0, and tetanic forces of both wt and *mdx* being lower than those previously found in younger mice.<sup>36</sup> Our result is in agreement with the age-dependent decrease of specific tetanic tension described in wt and *mdx* mice older than 10 months, with sP0 values of wt mice progressively becoming closer to those observed in age-matched *mdx*.<sup>37,44</sup> Almost no protective effect was exerted by taurine in *mdx* mice muscles, with only a slight improvement in sPt<sub>w</sub> and sP0 in DIA (Fig 5, A and B; recovery scores: sPt<sub>w</sub> = 23.6%, sP0 = 25.1%) and in sPt<sub>w</sub> in EDL muscle (Fig 5, C; recovery score: 19.5%). A trend toward amelioration was observed in the percentage of force reduction after eccentric contraction in EDL muscles from both wt and *mdx* mice treated with taurine, with respect to their untreated counterparts, although it was not significant (taurine-treated vs vehicle-treated wt mice:  $0.22\% \pm 2.1\%$  vs  $-8.1\% \pm 3.4$ ,  $n = 5$ ; taurine-treated vs vehicle-treated *mdx* mice:  $-41.6\% \pm 5.7$  vs  $-51.5\% \pm 3.8$ ,  $n = 5$ ).

**Effects of long-term taurine treatment on histopathology of heart and gastrocnemius muscle.** Representative images of cardiac muscle sections of treated and/or untreated wt and *mdx* mice are shown in Fig 6, A. While hearts of wt mice, either treated or not, showed no signs of histopathology, cardiac sections of *mdx* mice exhibited progressive interstitial fibrosis, polymorphic cardiomyocyte size, pleomorphic nuclei and cardiomyocyte degeneration. In particular, large areas of necrotic myocytes with infiltrating mononuclear cells were present. Interestingly in taurine-treated *mdx* mice hearts, there was a reduction of these histopathology signs (Fig 6, A). Qualitative results were supported by morphometric analysis, which showed a significant decrease (~70%) in the percentage of total area of damage (considered as the sum of necrosis, infiltration, and non-muscle area), and in particular of both infiltrates and of non-muscle tissue (Fig 6, B). In Fig 7, A are shown representative images of GC muscle sections from the different experimental groups. The typical hallmarks of dystrophic histopathology were clearly evident in *mdx* muscle sections, characterized by the presence of altered tissue architecture and of centronucleated myofibers, and by evident areas of non-muscle tissue, likely due to the deposition of fibrotic and adipose tissue. The presence of infiltrates was still detectable. Morphometric analysis revealed that taurine induced a general amelioration of the histopathological profile in *mdx* GC muscles reducing, although not significantly, the total area of damage by 34% (Fig 7, B). In particular, a significant reduction of infiltrates was observed in taurine-treated *mdx* mice ( $4.96 \pm 1.37\%$ , n samples/n of fields = 5/25) with respect to untreated ones ( $8.81 \pm 0.73$ , n samples/n of fields = 5/25;  $P < 0.008$ ).

Accordingly, taurine-treated *mdx* mice also showed a significant reduction in the percentage of centronucleated fibers ( $33.71 \pm 1.5\%$ , n samples/n of fields = 5/25) with respect to untreated ones ( $54.1 \pm 4.2\%$ , n samples/n of fields = 5/25;  $P < 0.005$ ). As expected, in *mdx* mice the cross-sectional area was significantly reduced to  $1502 \pm 141 \mu\text{m}^2$ , compared to  $2113 \pm 156 \mu\text{m}^2$  observed in wt animals. However, no effect of taurine on this parameter was observed either in wt or *mdx* muscles.

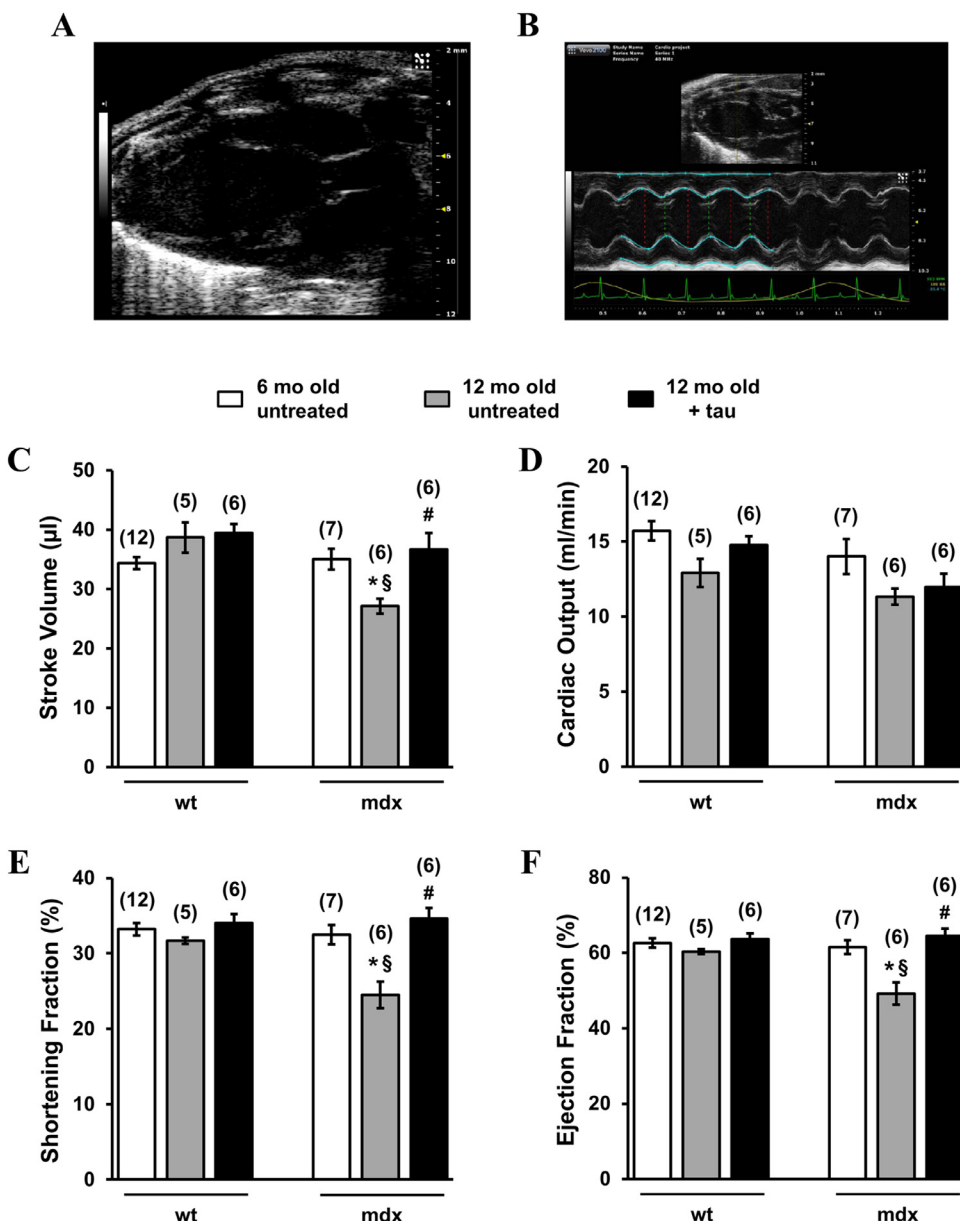


**Fig 2.** Cardiac ultrasonography. In **A** and **B** are shown representative pictures acquired during echocardiography on a wt mouse. In detail, **A** shows an image of the left ventricle acquired in B-mode by using the modified PLAX view, while **B** shows an image acquired in M-mode, placing the M-mode axis under the papillary muscle. Blue lines show how the measurements were performed to obtain the investigated cardiac parameters. In **C**, **D**, **E** and **F** is shown the modification of the main echocardiographic parameters in wt and *mdx* mice, before and after taurine administration. Each bar is the mean  $\pm$  SEM from the number of mice indicated in brackets. A significant difference among groups was found by ANOVA analysis for stroke volume ( $F = 7.6$ ;  $P < 0.002$ ), ejection fraction ( $F = 12$ ;  $P < 0.0002$ ) and shortening fraction ( $F = 12.6$ ;  $P < 0.0001$ ). Bonferroni post hoc correction for individual differences between groups is as follows: significantly different  $\S$  vs 6-months of age (6 mo old) untreated *mdx* mice ( $P < 0.002$ ); \*vs 12-months of age (12 mo old) untreated wt mice ( $P < 0.002$ ); #vs 12-months of age (12 mo old) untreated *mdx* mice ( $2.9 \times 10^{-5} < P < 0.004$ ).

**Effect of long-term taurine treatment on gene expression profile.** Quantitative Real-time PCR experiments were performed in heart samples to assess the impact of taurine treatment on expression of selected genes correlated to pathology progression and/or

mechanism of action. We found that cardiac IL-6 was significantly increased by 2.6-fold in untreated *mdx* with respect to untreated wt mice. Taurine treatment induced a significant reduction of 49% of IL-6 expression in *mdx* mice with respect to untreated ones,

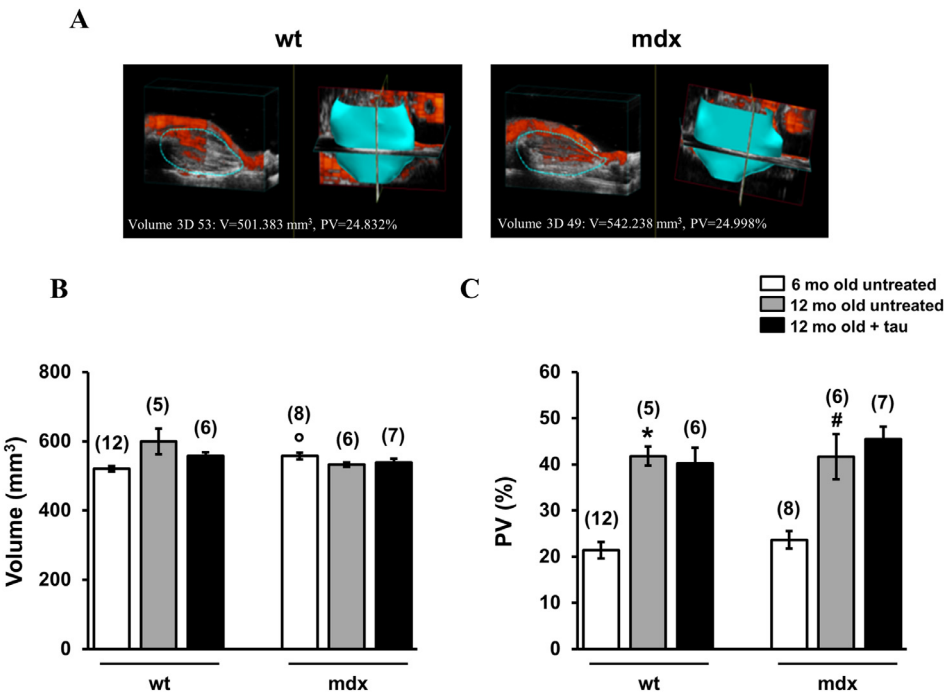


**Fig 3.** Modification of hind limb ultrasound parameters in wt and *mdx* mice, before and after taurine administration. In A is shown a sample image of 3D images of volume and percentage of vascularization reconstructed from the acquired 2D images using 3D Visualsonics software in wt (left panel) and *mdx* (right panel) mice. In B and C, the values for hind limb volume ( $\text{mm}^3$ ) and percentage of vascularization (PV, %) are shown. Each bar is the mean  $\pm$  SEM from the number of mice indicated in brackets. A significant difference among groups was found by ANOVA analysis for volume ( $F=5.28$ ,  $P \leq 0.05$ ) and PV ( $F=17.4$ ,  $P < 1.76 \times 10^{-6}$ ). Bonferroni post hoc correction for individual differences between groups is as follows: \*vs 6-months of age (6 mo old) untreated wt mice ( $P < 0.05$ ); \*vs 6-months of age (6 mo old) untreated wt mice ( $P < 1.32 \times 10^{-5}$ ); #vs 6-months of age (6 mo old) untreated *mdx* mice ( $P < 8 \times 10^{-5}$ ).

while no effect was observed in wt mice (Fig 8, A). We then analyzed the expression of the *Slc6a6* gene, encoding for taurine transporter (TauT) in the heart. No differences between genotypes were detected. The treatment with taurine did not induce any change of TauT expression in wt, but determined an overexpression by 42%, in the heart of *mdx* mice (Fig 8, B). Considering the role of taurine on mitochondrial metabolism,<sup>8</sup> we also assessed its effect on the expression of genes related to mitochondrial metabolism and in particular citrate synthase (Cs) and cytochrome c oxidase subunit IV isoform 1 (Cox4i1), key enzymes upstream and downstream the respiratory chain, respectively. No remarkable genotype-related differences were detected in basal gene expression. Cs expression was increased, although not significantly, by taurine administration in both wt (8%) and *mdx* (30%) mice. Also, taurine treatment induced an enhancement of the Cox4i1 gene expression in wt mice (13%) which became significant in *mdx* mice (41%) (Fig 8, B).

**Effect of long-term taurine administration on biochemical markers of muscle damage and on organ weight.** In *mdx* mice, the high plasma levels of CK and LDH enzymes are indices of sarcolemmal fragility and metabolic sufferance, respectively.<sup>11</sup> As shown in Fig 9, our study confirmed markedly higher plasma concentrations of both enzymes in 12-month-old dystrophic mice with respect to wt animals. The long-term treatment with taurine did not modify CK or LDH levels in wt mice (Fig 9, A and B). In agreement with previous observations, taurine confirmed its ability to significantly reduce high plasma

LDH in *mdx* mice (Fig 9, B), while only slightly decreased CK activity (Fig 9, A).<sup>18</sup>

Although taurine is a natural and safe compound, to exclude any sign of toxicity due to long-term administration of the amino acid, the masses of vital organs (liver, heart, kidney, and spleen) were measured and normalized to the body weight of each animal (mg/g). No significant differences were found for organ weights among the experimental groups (Table I).

**Taurine concentrations in skeletal muscle, internal organs, and plasma.** Taurine levels were measured by HPLC in quadriceps, heart, brain, liver, and plasma samples from treated and/or untreated wt and *mdx* groups (Fig 10). Significantly lower concentrations of taurine (about 50% less) were found in both skeletal and cardiac muscles from *mdx* mice compared to those from wt animals (Fig 10, A and B), while no significant differences between genotypes were observed in brain and liver samples (Fig 10, C and D). In parallel, untreated *mdx* plasma samples showed significantly higher levels of taurine with respect to wt mice ones (Fig 10, E). Taurine administration induced a slight, non-significant increase of taurine concentrations in heart and quadriceps of both wt and dystrophic mice (Fig 10, A and B), while almost no variation was observed in brain and liver of the treated groups (Fig 10, C and D). Interestingly, a significant increase in taurine levels was observed in plasma samples from treated wt mice with respect to their untreated counterparts, while a trend toward decrease was found in treated *mdx* mice with respect to vehicle-treated ones (Fig 10, E).

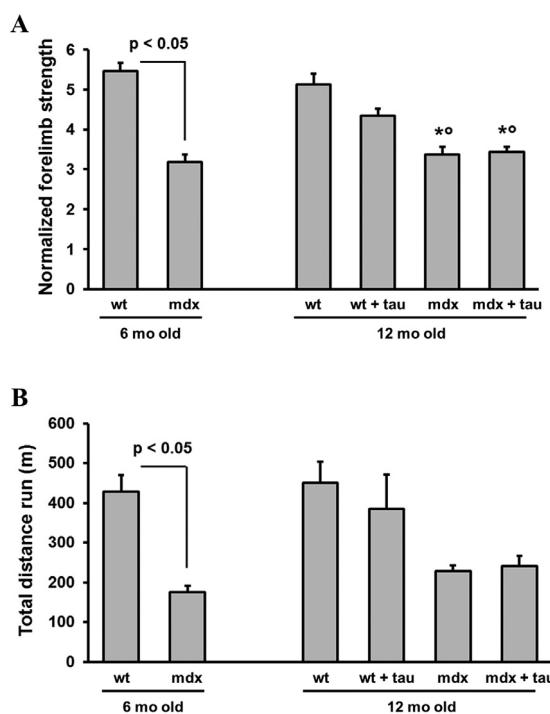


**Fig 4.** *In vivo* parameters of mouse force and fatigability in wt and *mdx* mice, before and after taurine administration. Each graph shows forelimb grip strength normalized on body weight (**A**) and total distance run during an exhaustion test on treadmill (**B**) at the beginning (6 mo old) and at the end (12 mo old) of the treatment for treated and/or untreated wt and exercised *mdx* mice. Each bar is the mean  $\pm$  SEM from 6 to 7 mice per group. In **A** and **B**, a significant difference among groups was found at 12 months of age by ANOVA analysis ( $F > 3.6$ ;  $P < 0.03$ ). In **A**, Bonferroni post hoc correction is as follows: significantly different with respect to \*wt ( $4.3 \times 10^{-6} < P < 7.5 \times 10^{-6}$ ), °wt + tau ( $0.002 < P < 0.004$ ). Intra- and inter-genotype significances found by unpaired Student's *t* test are indicated above the bars.

## DISCUSSION

Our study was the first *in vivo* and *ex vivo* preclinical evaluation of the effects of a long-term taurine administration on cardiac and skeletal muscle function in the *mdx* mouse model of DMD in comparison with age-matched wt mice. Most notably, we disclosed for the first time that our chronic treatment with this natural amino acid is useful in preventing, rather than simply reducing, late heart dysfunction in *mdx* mice. Taurine was administered (1 g/kg/day, in drinking water) to wt and *mdx* mice from 6 months of age, prior to the typical appearance of heart failure in dystrophic animals, which takes place around 9 months.<sup>28</sup> As revealed by our ultrasound evaluation of left ventricular function, the long-term treatment with taurine was able to induce a significant amelioration of the main indices related to myocardial contractility dysfunction (SF, EF, and SV) in *mdx* mice. The cardiac parameters in taurine-treated

*mdx* mice almost overlapped those found in wt mice, treated or not with taurine. This effect was not observed for CO, calculated as heart rate  $\times$  SV. The non-significant inter-genotype differences of CO and the limited effect of taurine on this parameter are most likely due to a high inter-individual variability and to the differences in heart rate among the experimental groups. In fact, heart rates of untreated wt and taurine-treated *mdx* mice were slightly lower than the heart rate of untreated *mdx* mice (wt: 344.3 bpm; untreated *mdx*: 422.5 bpm; *mdx* treated with taurine: 330 bpm). Although all values were perfectly within the range of normality for a murine model (300–400 bpm), we cannot rule out that the increase in heart rate in untreated *mdx* mice is in fact part of a compensatory sympathetic stimulation as typically occurs in early heart failure conditions.<sup>33</sup> In line with echocardiography results, we found that taurine administration ameliorated heart histologic profile, with a significant reduction of the percentage of total area of damage and in particular of infiltration and non-muscle tissue area. Gene expression analysis on cardiac muscle supported the view that taurine may exert a positive anti-inflammatory action, as shown by its ability to contrast the elevated expression of IL-6. Importantly, IL-6 has been indicated to play a complex role in the establishment of heart failure and cardiac damage, and it is indicated as a useful marker of cardiac pathology.<sup>45,46</sup> Then, the observed increase of IL-6 in *mdx* heart and its reduction in taurine-treated animals directly correlate with the functional and histological results.<sup>4,14</sup> In spite of the great impact observed on heart, the long-term treatment with taurine did not modify the skeletal muscle properties of either wt or *mdx* mice, as evidenced by the ultrasound evaluation of hind limb volume and percentage of vascularization. This was paralleled by *in vivo* results obtained after functional assessment of mouse forelimb grip strength and resistance to exercise, showing that in these experimental settings and mouse age range, taurine was not able to counteract *mdx* mice weakness and fatigability. These evidences were further confirmed by *ex vivo* contraction recordings of diaphragm and EDL muscle, both severely compromised in the dystrophic pathology also at this stage.<sup>11,47</sup> In addition, the treatment did not induce significant modifications of these parameters in the physiological condition represented by wt mice. Taken together and compared with previous results obtained in our short-term studies on exercised *mdx* mice,<sup>14,15,17,18</sup> these data suggest that taurine supplementation is probably more effective in an earlier, active phase of dystrophic pathology, characterized by acute muscle damage with frequent degeneration and/or regeneration cycles and more important inflammatory reaction.<sup>21,48</sup> In fact, in our earlier

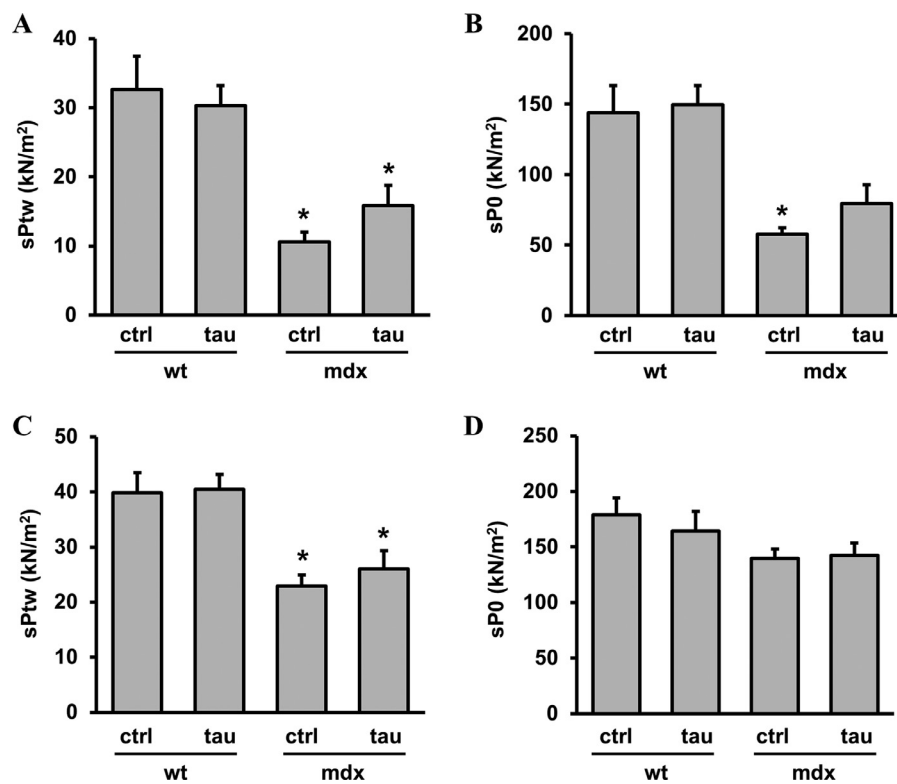


**Fig 5.** Effects of taurine treatment on *ex vivo* force of isolated muscles. In A and B are shown the normalized values of maximal isometric twitch (A, sPtw measured in kN/m<sup>2</sup>) and tetanic (B, sP0 measured in kN/m<sup>2</sup>) tensions of diaphragm strips from treated (tau) and/or untreated (ctrl) wt and *mdx* mice. Each bar is the mean  $\pm$  SEM from 4 to 7 mice per group. In C and D are shown the normalized values of sPtw (C) and sP0 (D) for *extensor digitorum longus* (EDL) muscle from the same experimental groups. In A, B, and C a significant difference among groups was found by ANOVA analysis ( $F > 9.5$ ,  $P < 0.0005$ ). Bonferroni post hoc correction for individual differences between groups is as follows: significantly different vs \*wt ( $0.0003 < P < 0.001$ ).

assessment in young exercised *mdx* mice, an improvement of muscle histology, along with a clear reduction of oxidative stress and inflammation biomarkers, was observed.<sup>18</sup> The slight protective effect on muscle histology observed in the present study, corroborates the complex relationship between structural and functional protection by taurine in dystrophic settings that may deserve further investigation. Then, it can be hypothesized that taurine can efficiently act in early mechanisms of dystrophy-related tissue damage, being less efficient in conditions of low-chronic disease stage. Alternatively, this latter state may alter some cellular mechanism involved in taurine action in skeletal muscle.

However, it is interesting to note that taurine confirmed its previously reported ability to significantly reduce high-plasma levels of LDH enzyme in *mdx* mice, but not those of CK.<sup>14,15,17,18</sup> LDH is a biochemical marker of the mechanical-metabolic sufferance typically observed in dystrophic animals. Thus, despite the poor efficacy of the long-term treatment on skeletal

muscle function, these results further support a role of taurine in positively influencing myofibers metabolism, through still unclear intracellular mechanisms that will deserve further investigations.<sup>4</sup>

In fact, some groups described no important changes in mitochondrial content at early *mdx* mouse age in relation to pathology severity, with no effect of taurine supplementation.<sup>49</sup> However, we have found that metabolic response of muscle to mechanical challenge, such as chronic exercise, is compromised, and this metabolic sufferance may increase with animal aging. In particular, a defect of mitochondrial adaptive response and of complex I has been described<sup>41,50</sup>; a complex interplay may occur between the above alterations and taurine in contractile tissues.

In fact, in mitochondria, taurine interaction with tRNA Leu (UUR), as well as with other tRNAs, plays a key role in complex I activity, promoting oxidative metabolism. In several mitochondrial disorders, the lack of taurine has been described to induce metabolic disturbance and cellular stress, impairing proper

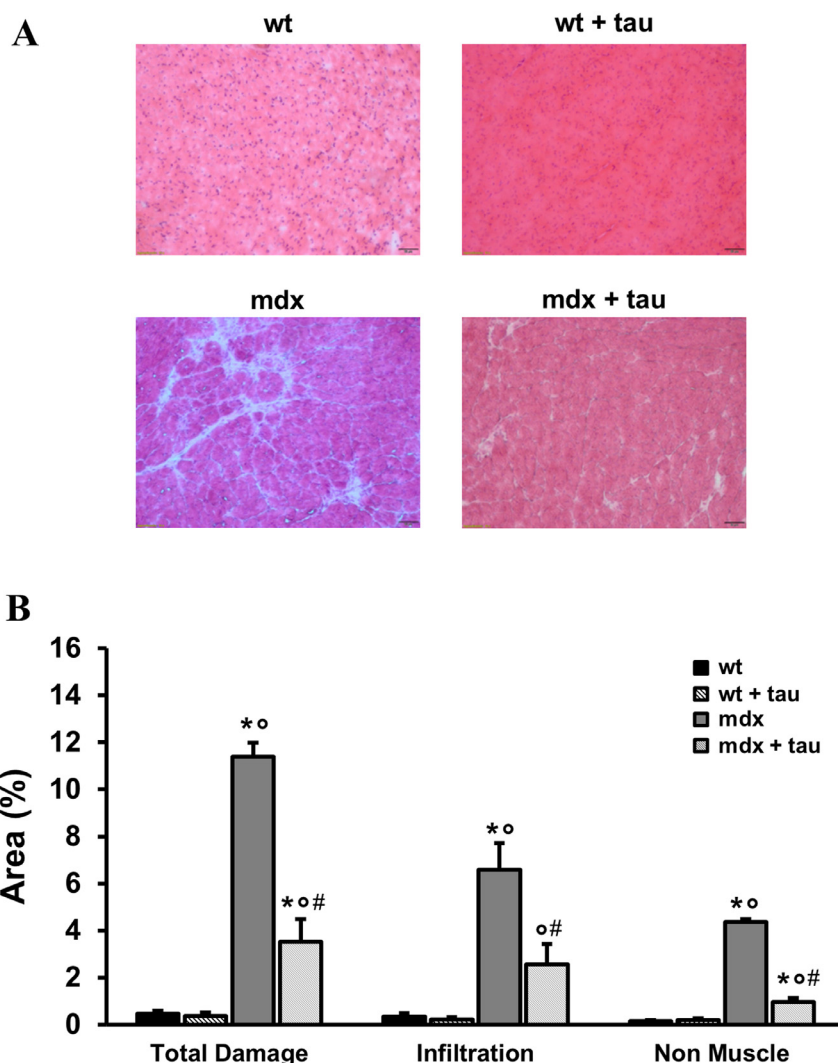


**Fig 6.** Effect of taurine administration on histological profile of cardiac muscle. In A are shown representative sections of hematoxylin & eosin-stained cardiac muscles (10 X magnification) from treated and/or untreated wt and *mdx* mice. In B is shown the calculated percentage of total area of damage, infiltration and non-muscle area from all the experimental groups. Each bar is the mean  $\pm$  SEM from at least 5 muscles and 5 fields for each muscle preparation. A significant difference among groups was found by ANOVA analysis ( $F > 17$ ,  $P < 8.8 \times 10^{-5}$ ). Bonferroni post hoc correction for individual differences between groups are as follows: significantly different vs \*wt ( $2.53 \times 10^{-11} < P < 0.002$ ), \*\*wt + tau ( $3.09 \times 10^{-11} < P < 0.008$ ), #*mdx* ( $3.76 \times 10^{-10} < P < 0.001$ ).

expression of proteins involved in respiratory chains and shifting toward a glycolytic profile.<sup>51–54</sup> Accordingly, in taurine-deficient hearts of TauTKO mice, Schaffer et al. have found an increase in glucose utilization by glycolysis and in lactate levels, but a reduction in glucose oxidation, this latter due to an impaired complex I activity.<sup>8</sup>

These observations open the attractive hypothesis that taurine fluctuation in *mdx* animals may contribute to some of the metabolic alterations observed in dystrophic tissues.<sup>50</sup> The reduction of LDH may actually confirm that taurine supplementation may partially rescue

a defective mitochondrial protein translation, similarly to what observed with the chaperone TUDC on lactate level, or positively act on the balance between aerobic and anaerobic metabolism, in favor of the former.<sup>52,54</sup> Importantly, Grounds et al. recently found that a deficiency in tRNAs levels in *mdx* skeletal muscles was rectified by taurine administration treated during postnatal growth, from 14 days to 3 weeks of age, the effect being more important at skeletal muscle level than in heart at this early stage.<sup>53</sup>

In line with this hypothesis, our data showed that the levels of the Cs and Cox4i1 genes, as markers of

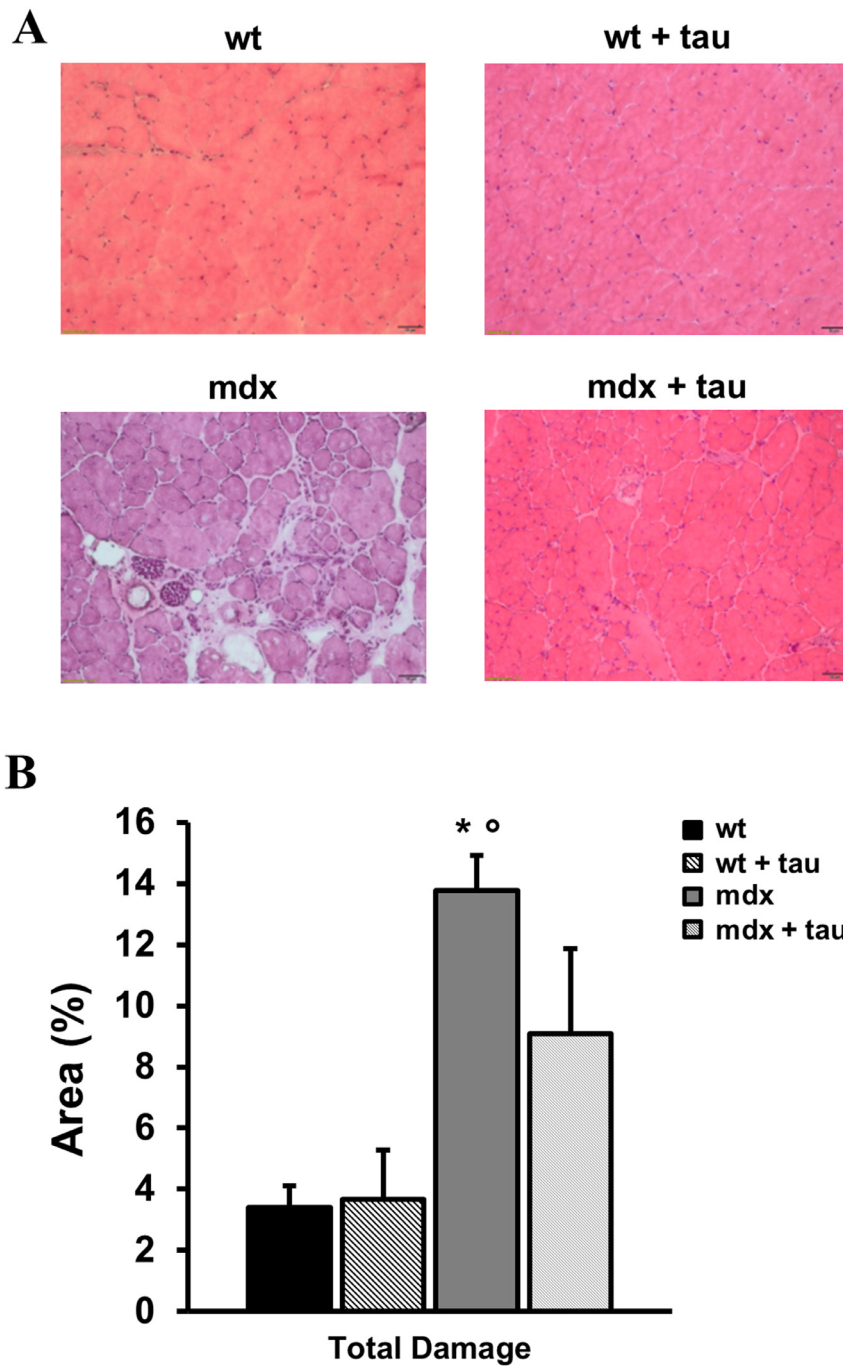


**Fig 7.** Effect of taurine administration on histological profile of gastrocnemius muscle. In A are shown representative sections of hematoxylin & eosin-stained gastrocnemius (GC) muscle (10 X magnification) from treated/untreated wt and *mdx* mice. In B is shown the calculated percentage of total area of damage from all the experimental groups. Each bar is the mean  $\pm$  SEM from at least 5 muscles and 5 fields for each muscle preparation. A significant difference among groups was found by ANOVA analysis ( $F = 7.96, P < 0.002$ ). Bonferroni post hoc correction for individual differences between groups are as follows: significantly different vs \*wt ( $P < 0.0007$ ), <sup>a</sup>wt + tau ( $P < 0.0008$ ).

mitochondria oxidative metabolism, were increased after taurine treatment. Interestingly, the enhancement of the expression levels of Cs and Cox4i1 was higher

in *mdx* mice with respect to wt further supporting the role of taurine in preventing the *mdx* heart damage by counteracting the metabolic shift.<sup>54</sup>

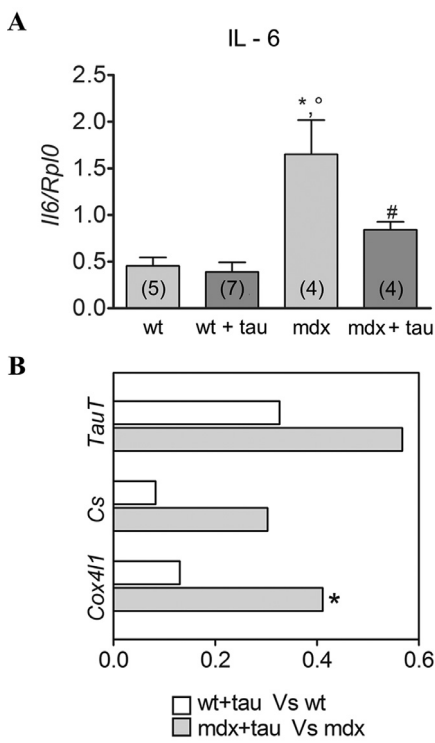


**Fig 8.** Effect of taurine treatment on cardiac expression of interleukin-6 (IL-6), taurine transporter (TauT), citrate syntase (Cs) and cytochrome c oxidase subunit IV isoform 1 (Cox4i1) genes. The histogram in A shows cardiac transcript levels with Real-time PCR of IL-6 normalized to ribosomal protein, large, P0 housekeeping gene (Rpl0) for all experimental groups. Each bar is the mean  $\pm$  SEM from the number of mice indicated in brackets. Significant differences between groups were evaluated using the one-way ANOVA test ( $F = 10.7$ ,  $P < 0.0005$ ). Bonferroni post hoc correction for individual differences between groups is as follows: significantly different ( $P < 0.05$ ) vs \*wt, \*wt + tau, #mdx. In B, transcript levels were determined by qPCR for TauT, Cs and Cox4i1 normalized to the RPL0 gene. The graphs show the effect of treatment in wt and mdx mice calculated as (wt + tau/wt)-1 in white bars (mdx + tau/mdx)-1 in gray bars. Each animal group was composed by 3–7 samples. \*Significant differences between groups by unpaired Student's *t* test ( $P < 0.05$ ).=

Along with this view, the hearts of TauTKO mice are characterized by enhanced apoptosis through mitochondria in young mice or via an increase of endoplasmic reticulum stress in older ones, along with alteration in phosphorylation in phospholamban and troponin that may contribute to heart.<sup>55,56</sup> Interestingly, the effects of taurine deficiency on mitochondrial apoptosis are blocked by the mitochondrial antioxidant, MitoTempo.<sup>55</sup>

The determination of taurine level after supplementation by HPLC disclosed that taurine distribution between plasma and tissues, in both basal conditions and after exogenous supplementation, is genotype-dependent. In

particular, taurine level significantly increased after supplementation in the plasma of wt animals, supporting the proper bioavailability of taurine formulation. In parallel, a modest tissue increase was observed in wt animals upon taurine treatment, opening the hypothesis that in conditions of physiological tissue level of the amino acid, the chronic administration of exogenous taurine may cause a compensatory adjustment to reduce the excess. This finding also opens to important consideration about the real interest of chronic supplement of taurine as energizer in physiological conditions and/or in the absence of age or exercise-related challenges.<sup>4</sup> By contrast, mdx mice had basal higher plasma level of taurine, likely in relation to the inability of the muscle to concentrate proper amino acid level, as supported by the significant reduction of taurine in both skeletal muscle and heart. This latter finding is in line with the marked reduction of taurine recently found by Terrill et al. in juvenile mdx mice<sup>21</sup> and represents a first-time observation in adult dystrophic animals, either treated or not with taurine. Alternative hypothesis for the higher plasma level can also envisage the activation of a compensatory mechanism, *i.e.* an increased synthesis in the liver. In fact, in brain and liver, no intra- or inter-genotype significant modifications of taurine levels were observed, although taurine concentrations in mdx mice livers, either treated or not, tended to be higher than in wt ones. Since the endogenous synthesis of taurine primarily occurs in the liver,<sup>2</sup> this may be related to the need of an increased amino acid synthesis in presence of taurine mishandling in dystrophic myofibers.<sup>13–15</sup> In both heart and quadriceps of mdx mice, a trend toward an increase of taurine levels versus wt level was found after the long-term treatment; in parallel an increase of TauT gene expression in heart of taurine-treated mdx mice compared to untreated mice was observed.

The inability of exogenous taurine administration to restore an adequate intracellular level of the amino acid in dystrophic tissues, in spite of the marked suffering, is surprising and in contrast with what observed in young mdx mice treated for 4 weeks.<sup>17</sup> A likely hypothesis could be related to the different basal conditions due to age and to the use of the exercise protocol, as well as to the duration of the treatment and the co-administration with PDN.<sup>17</sup> Also, the high level of muscle fibrosis which characterizes the advanced phase of the pathology, could limit the capacity of dystrophic myofibers to internalize taurine.<sup>4,11</sup> This could also be related to the establishment of a time-dependent adaptation mechanism involving the specific TauT transporter or to a progressive alteration of the equilibrium between amino acid absorption and/or excretion in mdx muscles. However, the data disclose the puzzling effect of taurine according to the stage of the disease and the duration of

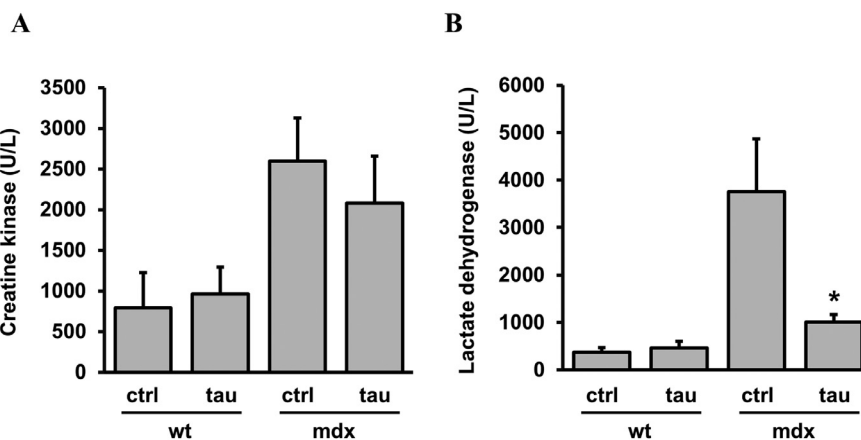


**Fig 9.** Plasma levels of creatine kinase (CK) and lactate dehydrogenase (LDH). In the figure are shown the levels of CK (A) and LDH (B) measured by spectrophotometry in plasma samples from treated (tau)/untreated (ctrl) wt and *mdx* mice expressed in units per liter (U/L). Each bar is the mean  $\pm$  SEM from 4 to 6 mice per group. For LDH significant difference among groups was found by ANOVA analysis ( $F = 5.20, P < 0.001$ ). No individual differences between groups were found by Bonferroni post hoc correction. \*Significantly different vs untreated *mdx* by unpaired Student's *t* test.

the supplementation. In addition, the present results show that the modest increase in tissue taurine level correlates in a complex manner with the *in vivo/ex vivo* functional parameters in heart vs muscle. In the light of this, we cannot exclude that the effects of taurine could be at least in part due to hydrogen sulfide ( $H_2S$ ) produced by taurine metabolism which has been demonstrated to exert protective effects in several types of cardiovascular disorders.<sup>57</sup> However, it is interesting to notice that the modest increase of taurine levels in the heart upon chronic administration was accompanied by a marked prevention of cardiac dysfunction. In agreement with previous hypothesis, this may be related to the early supplementation of taurine with respect to the development of cardiac dysfunction, *i.e.* at 6 months of age, suggesting that taurine may delay or contrast the action of harmful factors contributing to the development of cardiac failure.<sup>58</sup>

All together, these observations suggest a pharmacological action of taurine in dystrophic tissues that is pivotal in early induction mechanisms of heart dysfunction and damage, such as oxidative stress and

inflammation.<sup>58</sup> This action may in part depend by appropriate tissue concentration leading to hypothesize alternative site of action, such as neutrophils and macrophages, as source of reactive oxygen species (ROS) and organ damage, as recently proposed by Terrill et al., in a focused study on canine model of DMD.<sup>20</sup> The present results pave the way to further studies to gain more insight into the mechanisms through which taurine exerts its positive effects at cardiac level, as well as in the amount of protection that can be obtained at both muscle and cardiac level with a life long-term taurine treatment. Alternatively, supplementation of taurine tailored on disease phase may help to better address its therapeutic action of affected tissues.

Finally, our result can be considered as clinically relevant, in relation to the importance assumed by cardiovascular health management in DMD patients. The possibility of a chronic administration of a safe compound as taurine to prevent dilated cardiomyopathy in boys affected by Duchenne (or Becker) muscular dystrophy could be a great opportunity to ameliorate both their life quality and expectancy.<sup>59</sup>

**Table I.** Effect of taurine on vital organs. The table shows the weights of vital organs (liver, heart, kidney, and spleen), normalized on the body weight of each mouse (mg/g). Each value is expressed as the mean  $\pm$  SEM from the number of mice indicated in the column. A significant difference among groups was found by ANOVA analysis for liver ( $F = 3.3, P < 0.04$ ) and spleen ( $F = 4.9, P < 0.01$ ). No significant differences between individual values were found by Bonferroni post hoc correction.

n	Liver (mg/g)	Heart (mg/g)	Kidney (mg/g)	Spleen (mg/g)	
wild type	6	44.6 $\pm$ 1.3	5.7 $\pm$ 0.3	7.4 $\pm$ 0.8	4.2 $\pm$ 0.2
wild type + taurine	7	46.3 $\pm$ 2.1	5 $\pm$ 0.1	7.4 $\pm$ 0.2	4 $\pm$ 0.3
<i>mdx</i>	6	57.3 $\pm$ 3.9	5.5 $\pm$ 0.3	8.1 $\pm$ 0.5	3.3 $\pm$ 0.2
<i>mdx</i> + taurine	6	51 $\pm$ 4.3	6.1 $\pm$ 0.4	8.3 $\pm$ 0.5	3.1 $\pm$ 0.2

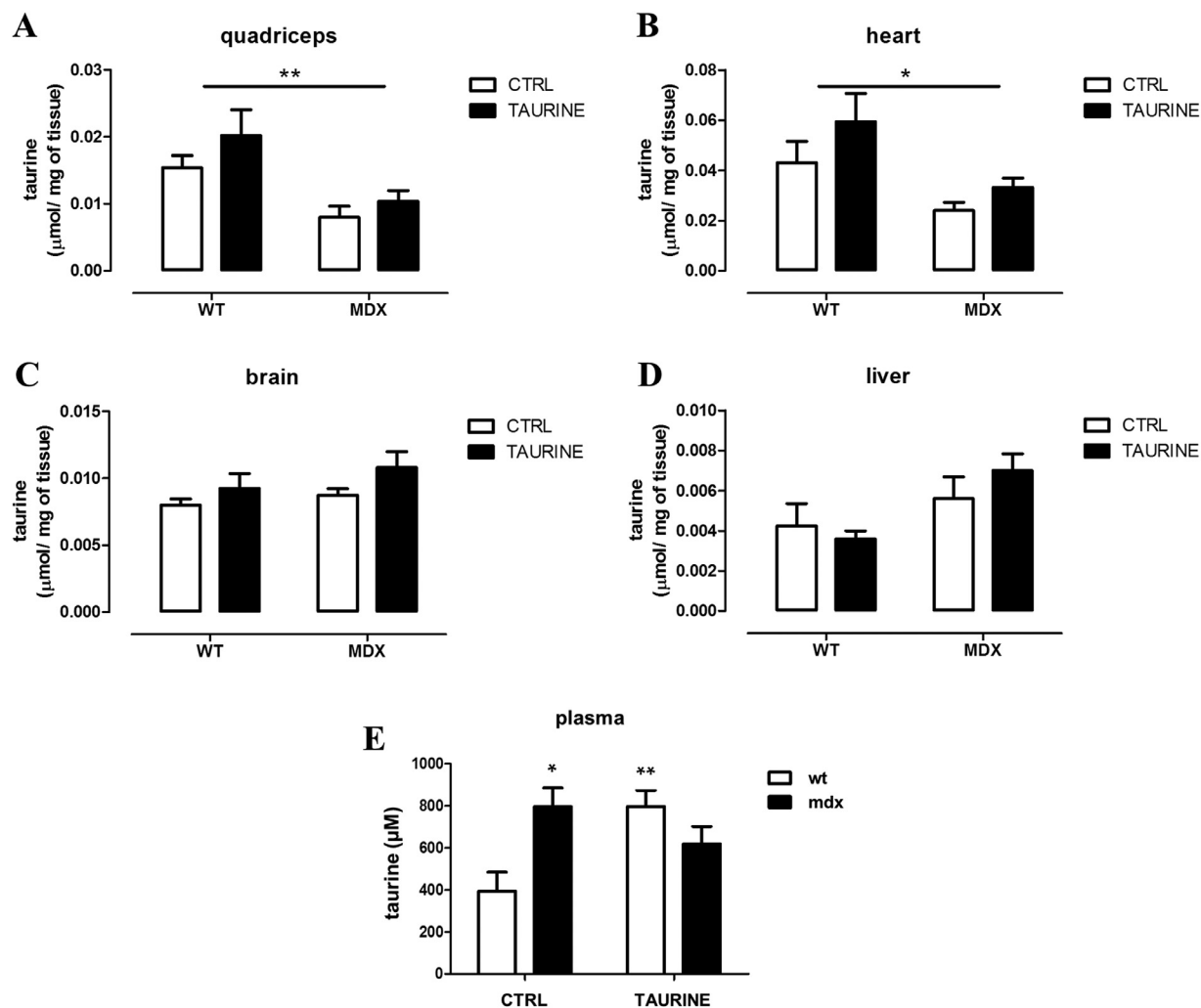


**Fig 10.** Taurine concentrations in skeletal muscle, internal organs and plasma. In the figure are shown the levels of taurine measured by high performance liquid chromatography (HPLC) in quadriceps muscle (**A**), heart (**B**), brain (**C**), liver (**D**) expressed in  $\mu\text{mol}/\text{mg}$ , and in plasma samples ( $\mu\text{M}$ , **E**) from treated (taurine)/untreated (ctrl) wt and *mdx* mice. In A, B, and E statistically significant differences among groups were found by ANOVA analysis. Bonferroni post hoc correction for individual differences between groups is as follows: significantly different vs wt mice (\* $P < 0.05$ ; \*\* $P < 0.01$ ).

#### ACKNOWLEDGMENTS

Conflicts of Interest: All authors have read the journal's policy on disclosure of potential conflicts of interest and have none to declare. All authors have read the journal's authorship agreement, and the manuscript has been reviewed by and approved by all named authors. No editorial support was used for preparation of the manuscript.

The research has been supported by PRIN-MIUR (Research Projects of National Interest – Ministry of Education, University and Research) project no. 20108YB5W3\_004 and The Dutch Duchenne Parent Project NL (DPP NL).

A.M., P.M., and A.D.L. developed the hypothesis and designed the experiments. A.M., P.M., M.D.B., F.R., F.S., E.C., M.G.M., M.B., R.F.C., S.P. and G.M.C. performed the experiments and analyzed the results. A.M., P.M., J.F.R., L.T., and A.D.L. reviewed the results and prepared the manuscript.

#### REFERENCES

1. Steele DS, Smith GL, Miller DJ. The effects of taurine on  $\text{Ca}^{2+}$  uptake by the sarcoplasmic reticulum and  $\text{Ca}^{2+}$  sensitivity of chemically skinned rat heart. *J Physiol* 1990;422:499–511.
2. Huxtable RJ. Physiological actions of taurine. *Physiol Rev* 1992;72:101–63.

3. Schaffer S, Ju Jong C, Kc R, Azuma J. Physiological roles of taurine in heart and muscle. *J Biomed Sci* 2010;17:S2.
4. De Luca A, Piero S, Camerino DC. Taurine: the appeal of a safe amino acid for skeletal muscle disorders. *J Transl Med* 2015;13:243.
5. Ito T, Oishi S, Takai M, et al. Cardiac and skeletal muscle abnormality in taurine transporter-knockout mice. *J Biomed Sci* 2010;17(Suppl 1):S20.
6. Warskulat U, Heller-Stilb B, Oermann E, et al. Phenotype of the taurine transporter knockout mouse. *Methods Enzymol* 2007;428:439–58.
7. Ito T, Kimura Y, Uozumi Y, et al. Taurine depletion caused by knocking out the taurine transporter gene leads to cardiomyopathy with cardiac atrophy. *J Mol Cell Cardiol* 2008;44:927–37.
8. Schaffer SW, Shimada-Takaura K, Jong CJ, Ito T, Takahashi K. Impaired energy metabolism of the taurine-deficient heart. *Amino Acids* 2016;48:549–58.
9. Piero S, De Luca A, Huxtable RJ, Conte Camerino D. Dual effects of taurine on membrane ionic conductances of rat skeletal muscle fibers. *Adv Exp Med Biol* 1994;359:217–24.
10. De Luca A, Piero S, Camerino DC. Effect of taurine depletion on excitation-contraction coupling and  $\text{Cl}^-$  conductance of rat skeletal muscle. *Eur J Pharmacol* 1996;296:215–22.
11. Grounds MD, Radley HG, Lynch GS, Nagaraju K, De Luca A. Towards developing standard operating procedures for pre-clinical testing in the mdx mouse model of Duchenne muscular dystrophy. *Neurobiol Dis* 2008;31:1–19.
12. Hoffman EP, Dressman D. Molecular pathophysiology and targeted therapeutics for muscular dystrophy. *Trends Pharmacol Sci* 2001;22:465–70.
13. McIntosh LM, Granberg KE, Briere KM, Anderson JE. Nuclear magnetic resonance spectroscopy study of muscle growth, mdx dystrophy and glucocorticoid treatments: correlation with repair. *NMR Biomed* 1998;11:1–10.
14. De Luca A, Piero S, Liantonio A, Cetrone M, Camerino C, Simonetti S, et al. Alteration of excitation–contraction coupling mechanism in extensor digitorum longus muscle fibres of dystrophic mdx mouse and potential efficacy of taurine. *Br J Pharmacol* 2001;132:1047–54.
15. De Luca A, Piero S, Liantonio A, et al. Enhanced dystrophic progression in mdx mice by exercise and beneficial effects of taurine and insulin-like growth factor-1. *J Pharmacol Exp Ther* 2003;304:453–63.
16. Terrill JR, Grounds MD, Arthur PG. Taurine deficiency, synthesis and transport in the mdx mouse model for Duchenne Muscular Dystrophy. *Int J Biochem Cell Biol* 2015;66:141–8.
17. Cozzoli A, Rolland JF, Capogrosso RF, et al. Evaluation of potential synergistic action of a combined treatment with alpha-methyl-prednisolone and taurine on the mdx mouse model of Duchenne muscular dystrophy. *Neuropathol Appl Neurobiol* 2011;37:243–56.
18. Capogrosso RF, Cozzoli A, Mantuano P, et al. Assessment of resveratrol, apocynin and taurine on mechanical-metabolic uncoupling and oxidative stress in a mouse model of duchenne muscular dystrophy: a comparison with the gold standard,  $\alpha$ -methyl prednisolone. *Pharmacol Res* 2016;106:101–13.
19. Terrill JR, Boyatzis A, Grounds MD, Arthur PG. Treatment with the cysteine precursor 1,2-oxothiazolidine-4-carboxylate (OTC) implicates taurine deficiency in severity of dystrophopathy in mdx mice. *Int J Biochem Cell Biol* 2013;45:2097–108.
20. Terrill JR, Duong MN, Turner R, et al. Levels of inflammation and oxidative stress, and a role for taurine in dystrophopathy of the Golden Retriever Muscular Dystrophy dog model for Duchenne Muscular Dystrophy. *Redox Biol* 2016;9:276–86.
21. Terrill JR, Pinniger GJ, Nair KV, Grounds MD, Arthur PG. Beneficial effects of high dose taurine treatment in juvenile dystrophic mdx mice are offset by growth restriction. *PLoS One* 2017;12:e0187317.
22. Ghandforoush-Sattari M, Mashayekhi S, Krishna CV, Thompson JP, Routledge PA. Pharmacokinetics of oral taurine in healthy volunteers. *J Amino Acids* 2010;2010:346237.
23. Lourenço R, Camilo ME. Taurine: a conditionally essential amino acid in humans? An overview in health and disease. *Nutr Hosp* 2002;17:262–70.
24. Nigro G, Comi LI, Politano L, Bain RJ. The incidence and evolution of cardiomyopathy in Duchenne muscular dystrophy. *Int J Cardiol* 1990;26:271–7.
25. Connuck DM, Sleeper LA, Colan SD, et al. Characteristics and outcomes of cardiomyopathy in children with Duchenne or Becker muscular dystrophy: a comparative study from the Pediatric Cardiomyopathy Registry. *Am Heart J* 2008;155:998–1005.
26. Xu Y-J, Arneja AS, Tappia PS, Dhalla NS. The potential health benefits of taurine in cardiovascular disease. *Exp Clin Cardiol* 2008;13:57–65.
27. Bakrania B, Du Toit EF, Wagner KH, Headrick JP, Bulmer AC. Pre- or post-ischemic bilirubin ditaurate treatment reduces oxidative tissue damage and improves cardiac function. *Int J Cardiol* 2016;202:27–33.
28. Shirokova N, Niggli E. Cardiac phenotype of Duchenne Muscular Dystrophy: insights from cellular studies. *J Mol Cell Cardiol* 2013;58:217–24.
29. Capogrosso RF, Mantuano P, Uaesoontrachoon K, et al. Ryanodine channel complex stabilizer compound S48168/ARM210 as a disease modifier indystrophin-deficient mdx mice: proof-of-concept study and independent validation of efficacy. *FASEB J*. 2018;32:1025–43.
30. De Luca A, Nico B, Liantonio A, et al. A multidisciplinary evaluation of the effectiveness of cyclosporine in dystrophic mdx mice. *Am J Pathol* 2005;166:477–89.
31. Mele A, Fonzino A, Rana F, et al. In vivo longitudinal study of rodent skeletal muscle atrophy using ultrasonography. *Sci Rep* 2016;6:20061.
32. Conte E, Camerino GM, Mele A, et al. Growth hormone secretagogues prevent dysregulation of skeletal muscle calcium homeostasis in a rat model of cisplatin-induced cachexia. *J Cachexia Sarcopenia Muscle* 2017;8:386–404.
33. Spurny CF, Knoblauch S, Pistilli EE, Nagaraju K, Martin GR, Hoffman EP. Dystrophin-deficient cardiomyopathy in mouse: expression of Nox4 and Lox are associated with fibrosis and altered functional parameters in the heart. *Neuromuscul Disord* 2008;18:371–81.
34. Moorwood C, Liu M, Tian Z, Barton ER. Isometric and eccentric force generation assessment of skeletal muscles isolated from murine models of muscular dystrophies. *J Vis Exp* 2013(71): e50036.
35. Zanou N, Iwata Y, Schakman O, Lebacq J, Wakabayashi S, Gailly P. Essential role of TRPV2 ion channel in the sensitivity of dystrophic muscle to eccentric contractions. *FEBS Lett* 2009;583:3600–4.
36. Capogrosso RF, Mantuano P, Cozzoli A, et al. Contractile efficiency of dystrophic mdx mouse muscle: in vivo and ex vivo assessment of adaptation to exercise of functional endpoints. *J Appl Physiol. (1985)* 2017;122:828–43.
37. Brooks SV, Faulkner JA. Contractile properties of skeletal muscle of young, adult and aged mice. *J Physiol* 1988;404:71–82.
38. Burdi R, Rolland JF, Fraysse B, et al. Multiple pathological events in exercised dystrophic mdx mice are targeted by pentoxifylline: outcome of a large array of in vivo and ex vivo tests. *J Appl Physiol*. 2009;106:1311–24.

39. Mantuano P, Sanarica F, Conte E, et al. Effect of a long-term treatment with metformin in dystrophic mdx mice: a reconsideration of its potential clinical interest in Duchenne muscular dystrophy. *Biochem Pharmacol* 2018;154:89–103.
40. Bustin SA, Benes V, Garson JA, et al. The MIQE guidelines: minimum information for publication of quantitative real-time PCR experiments. *Clin Chem* 2009;55:611–22.
41. Camerino GM, Cannone M, Giustino A, et al. Gene expression in mdx mouse muscle in relation to age and exercise: aberrant mechanical-metabolic coupling and implications for pre-clinical studies in Duchenne muscular dystrophy. *Hum Mol Genet* 2014;23:5720–32.
42. Tucci P, Mhillaj E, Morgese MG, et al. Memantine prevents memory consolidation failure induced by soluble beta amyloid in rats. *Front Behav Neurosci* 2014;8:332.
43. Duddy W, Duguez S, Johnston H, et al. Muscular dystrophy in the mdx mouse is a severe myopathy compounded by hypotrophy, hypertrophy and hyperplasia. *Skelet Muscle* 2015;5:16.
44. Lynch GS, Hinkle RT, Chamberlain JS, Brooks SV, Faulkner JA. Force and power output of fast and slow skeletal muscles from mdx mice 6–28 months old. *J Physiol* 2001;535(Pt 2):591–600.
45. Kanda T, Takahashi T. Interleukin-6 and cardiovascular diseases. *Jpn Heart J* 2004;45:183–93.
46. Fontes JA, Rose NR, Čiháková D. The varying faces of IL-6: From cardiac protection to cardiac failure. *Cytokine* 2015;74:62–8.
47. Lynch GS, Rafael JA, Hinkle RT, Cole NM, Chamberlain JS, Faulkner JA. Contractile properties of diaphragm muscle segments from old mdx and old transgenic mdx mice. *Am J Physiol* 1997;272:C2063–8.
48. Terrill JR, Pinniger GJ, Graves JA, Grounds MD, Arthur PG. Increasing taurine intake and taurine synthesis improves skeletal muscle function in the mdx mouse model for Duchenne muscular dystrophy. *J Physiol* 2016;594:3095–110.
49. Barker RG, Wyckelsma VL, Xu H, Murphy RM. Mitochondrial content is preserved throughout disease progression in the mdx mouse model of Duchenne muscular dystrophy, regardless of taurine supplementation. *Am J Physiol Cell Physiol* 2018;314:C483–91.
50. Gamberi T, Fiaschi T, Valocchia E, et al. Proteome analysis in dystrophic mdx mouse muscle reveals a drastic alteration of key metabolic and contractile proteins after chronic exercise and the potential modulation by anti-oxidant compounds. *J Proteomics* 2018;170:43–58.
51. Suzuki T, Nagao A, Suzuki T. Human mitochondrial diseases caused by lack of taurine modification in mitochondrial tRNAs. *Wiley Interdiscip Rev RNA* 2011;2:376–86.
52. Fakrurraad M, Wei FY, Suzuki T, et al. Defective mitochondrial tRNA taurine modification activates global proteostress and leads to mitochondrial disease. *Cell Rep* 2018;22:482–96.
53. Butchart LC, Terrill JR, Rossetti G, White R, Filipovska A, Grounds MD. dExpression patterns of regulatory RNAs, including lncRNAs and tRNAs, during postnatal growth of normal and dystrophic (mdx) mouse muscles, and their response to taurine treatment. *Int J Biochem Cell Biol* 2018;99:52–63.
54. Schaffer SW, Jong CJ, Ito T, Azuma J. Role of taurine in the pathologies of MELAS and MERRF. *Amino Acids* 2014;46:47–56.
55. Jong CJ, Ito T, Prentice H, Wu JY, Schaffer SW. Role of mitochondria and endoplasmic reticulum in taurine-deficiency-mediated apoptosis. *Nutrients* 2017;9(8):pii: E795.
56. Ramila KC, Jong CJ, Pastukh V, Ito T, Azuma J, Schaffer SW. Role of protein phosphorylation in excitation-contraction coupling in taurine deficient hearts. *Am J Physiol Heart Circ Physiol* 2015;308:H232–9.
57. Liang B, Xiao T, Long J, Liu M, Li Z, Liu S, Yang J. Hydrogen sulfide alleviates myocardial fibrosis in mice with alcoholic cardiomyopathy by downregulating autophagy. *Int J Mol Med* 2017;40:1781–91.
58. Ito T, Schaffer S, Azuma J. The effect of taurine on chronic heart failure: actions of taurine against catecholamine and angiotensin II. *Amino Acids* 2014;46:111–9.
59. Bushby K, Finkel R, Birnkrant DJ. Diagnosis and management of Duchenne muscular dystrophy, part 1: diagnosis, and pharmacological and psychosocial management. *Lancet Neurol* 2010;9:77–93.